ISSN: 2414-1895 DOI: 10.6919/ICJE.202501_11(1).0002

Microstructure and Properties of CoCrFeNiTi-Ti_2AlC@Ni high-Entropy Alloy Composite Coatings by Ultra-high Speed Laser Cladding

Yunpeng Zhao

School of mechanical engineering, Tianjin University of Technology and Education, Tianjin 300222, China

Abstract

In this paper, the CoCrFeNiTi- Ti_2AlC@Ni high entropy alloy self-lubricating composite coating was prepared on the surface of Cr12MoV die steel by using the ultra-high speed laser cladding technology. Its phase composition, microstructure, element distribution, nano-hardness, wear resistance and anti-deformation ability were studied. The research results show that after adding Ti_2AlC into the coating, there are relatively significant changes in both its microstructure and mechanical properties. From the perspective of microstructure, under the action of Ti_2AlC, the grains are distributed more densely and uniformly, demonstrating good microstructure characteristics. In terms of mechanical properties, under the effect of grain refinement strengthening and the pinning effect of the newly generated phases, the indentation depth of the coating decreases from 1212 nm to 989 nm, and the elastic modulus increases from 204.06 Gpa to 228 Gpa, showing good resistance to plastic deformation. The nano-hardness of the coating increases from 8.65 Gpa to 12.57 Gpa. Moreover, Ti_2AlC plays a pivotal role in reducing friction during the friction process. Therefore, under the synergistic effect of high hardness and self-lubrication, the wear resistance of the coating is improved, and the wear resistance of the coating reaches the best when it is 3%. At this time, the wear scar is the narrowest and the shallowest, the coating wear is the most uniform, and the friction coefficient decreases from 0.528 to 0.481.

Keywords

Ultra-high Speed Laser Cladding; Self-lubricating Composite Coating; Cr12MoV Die Steel; Mechanical Properties; High Entropy Alloy.

1. Introduction

With the booming development of automobile industry, the annual output of automobiles has been increasing year by year, and the pace of renewal and upgrading has been continuously accelerating. Correspondingly, the demand for molds has also been on a continuous upward trend. Among a wide variety of mold materials, Cr12MoV die steel, as a traditional cold work die steel, has been widely applied in the field of cold stamping die manufacturing due to its relatively good comprehensive properties, such as high hardness, strength, and a certain degree of toughness. However, in actual use, molds often suffer from surface wear problems, which lead to a significant reduction in their service life and limit their applications in some key fields. It is extremely necessary to adopt surface modification technologies to repair and strengthen worn molds, reduce surface wear, and extend the service life of molds.

Traditional laser cladding, as a surface modification technology [1], can achieve the surface repair or strengthening of automobile molds. Its working principle is to melt the metal surface with a laser

ISSN: 2414-1895 DOI: 10.6919/ICJE.202501_11(1).0002

beam to form a micro-molten pool, spray metal powder into it, and finally form a new metal coating with special functions [2, 3]. Laser cladding technology has the advantages of free powder selection, the ability to precisely select areas, the capability to form a metallurgical bond with the substrate, a fast cooling speed of the prepared new metal coating, and easy automation of the cladding process [4]. Nevertheless, traditional laser cladding has limitations such as a large heat input rate to the substrate and low cladding efficiency, which, to some extent, restricts its application in the surface strengthening and repair of large components [5 - 7]. In order to further expand the application of laser cladding technology and solve problems such as large heat input and low cladding rate, researchers have discovered the ultra-high speed laser cladding technology. Compared with traditional laser cladding, the characteristic of ultra-high speed laser cladding technology is that the metal powder reaches a molten state before reaching the substrate [8]. It only forms a micro-molten pool on the substrate surface, reduces the heat input to the substrate and the dilution rate of the coating, and makes the cladding efficiency more than ten times that of traditional laser cladding [9,10]. In addition, the performance of the ultra-high speed laser cladding coating is also significantly better than that of the traditional laser cladding coating. Research shows that, compared with traditional laser cladding technology, the coating prepared by using ultra-high speed laser cladding technology can obtain higher hardness [11] and wear resistance [12].

In 2004, Yeh et al. [13, 14] proposed the concept of high entropy alloy (HEA). Due to the four major effects of high entropy alloys (high entropy effect, cocktail effect, lattice distortion effect, and sluggish diffusion effect), they possess relatively good high hardness and wear resistance properties [15]. Li et al. [16] prepared CoCrFeNiTix (x = 0, 0.25, 0.5, 0.75, 1.0) high entropy alloy coatings on 45# steel. The results showed that the addition of Ti caused the coating grains to be refined and led to severe lattice distortion, enhancing the solid solution strengthening effect of the coating and increasing the hardness of the coating by 2.3 times. Wang et al. [17] used laser cladding technology to prepare CoCrFeNiTix high entropy alloy coatings. The research found that with the increase in the content of Ti element, and new phases constantly emerged on the basis of the original FCC phase, such as the tetragonal FeCr phase, the rhombic NiTi phase, and the hexagonal CoTi phase. The increase in Ti content also led to the further growth of secondary dendrite arms and the reduction of the secondary dendrite arm spacing. Eventually, under the combined effect of lattice distortion and dispersion strengthening, the hardness of the coating increased by 2.83 times. However, with the rapid development of the automobile industry and the increasingly sophisticated mold manufacturing process, more stringent requirements have been put forward for the wear resistance and tribological characteristics of molds. In the actual use process of automobile molds, relying solely on the existing wear resistance of high entropy alloys is difficult to fully meet these complex and demanding working conditions. Taking this into account, the introduction of a lubricating phase has become a promising optimization strategy. The MAX phase, as a unique layered compound, has the high wear resistance characteristics of ceramic materials and the self-lubricating performance of layered compounds. Incorporating it into the high entropy alloy system as a lubricating phase to construct a composite coating can effectively reduce the friction coefficient between the coating and the friction pair and further improve the wear resistance of the coating. Zhou et al. [18] used laser cladding technology to fabricate WS_2 and Ti_3AlC_2 - enhanced YW1/NiCoCrAlY coatings on T - 4241 high - speed steel. The results showed that after adding WS_2 and Ti_3AlC_2, the friction coefficient of the coating decreased by 20.9% and 39.1%, respectively, and the corresponding wear rate decreased by 35.1% and 65.4%, respectively. The wear rate and friction coefficient of the coating with added Ti_3AlC_2 were the lowest because the coating with added Ti_3AlC_2 could form a continuous self - lubricating film during the wear process, which could play a good role in reducing friction. Li et al. [19] also used laser cladding technology to prepare Ti_3SiC_2/Co - based composite coatings. Research showed that under the synergistic effect of the MAX phase in the coating and the decomposed hard phases, the microhardness of the coating increased by 2.3 times, and the wear rate decreased by 84%. Research has proven that adding the MAX phase to the coating can achieve the purpose of reducing friction by using its special structure. However, at present, there are relatively few studies on adding a lubricating

ISSN: 2414-1895 DOI: 10.6919/ICJE.202501_11(1).0002

phase to high entropy alloys and investigating its influence on the tribological and mechanical properties of the coating, lacking more in - depth research and exploration.

Therefore, in order to make better use of the self - lubricating characteristics of the MAX phase, this paper adopts two high entropy alloys, namely, Ti_2AlC coated with nickel in a mixed way and CoCrFeNiTi, to prepare a coating with better self - lubricating performance and higher hardness, thus further extending the service life of molds. In this paper, Ti_2AlC is added to the CoCrFeNiTi high entropy alloy coating according to different mass ratios. The variation laws of the macro - quality, phase structure, microstructure, and mechanical properties of the coating are studied. By evaluating and comparing the changes in the microstructure, phase structure, and mechanical properties of the coating, the mechanism of the lubricating and friction - reducing effect of Ti_2AlC on the coating is revealed.

2. Experimental Materials and Methods

The CoCrFeNiTi powder and Ti_2AlC powder (as shown in Fig. 1) were proportioned according to the mass ratio, and then mechanically ball-milled and mixed in a planetary ball mill at a rotational speed of 300 r/min for 3 hours to obtain the CoCrFeNiTi- Ti_2AlC high entropy alloy powder. Subsequently, the obtained CoCrFeNiTi- Ti_2AlC high entropy alloy powder was placed in an oven and dried for later use. Then, the ultra-high speed laser device was used to prepare a high entropy alloy-based composite coating on the surface of Cr12MoV die steel. After the coating was prepared, it was cut into specimens with the size of 10 × 10 × 10 mm. Energy dispersive spectrometer (EDS) and scanning electron microscope (SEM) were adopted to analyze the microstructure and element distribution of the coating. The samples were subjected to a meticulous grinding and polishing procedure employing sandpapers whose grits ranged from P400 to P2000. Subsequently, the treated specimens were etched with aqua regia (in a volumetric ratio of HCl: HNO_3 = 3: 1) for the purpose of observing the microstructural organization of the etched samples. The hardness of the specimens was detected by using a Vickers microhardness tester. The applied load was set at 200 g, with a loading duration of 10 s. Moreover, the load was applied at intervals of 50 um as it was moved downward from the top of the coating's cross-section towards the substrate. The mechanical properties and fracture toughness of the coating were detected by using a nano-indentation instrument. The nano-indentation loading force was 200 mN, and the loading time was maintained for 10 seconds. Finally, the wear resistance of the coating was detected by using a Bruker multifunctional friction and wear tester. The specific parameters of the coating preparation process are shown in Table 1.

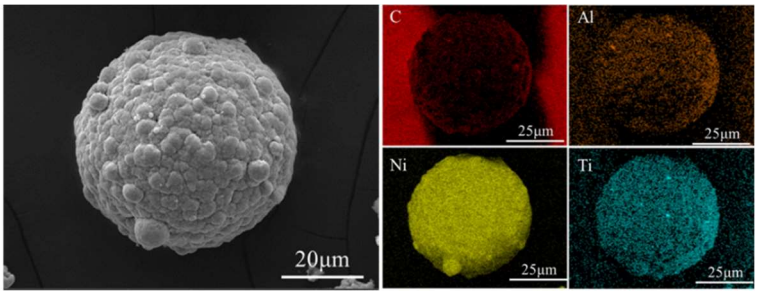

Fig. 1 Element Distribution of Ti_2AlC Powder

Table 1. Experimental process parameters

Laser power (w)	Scanning speed (mm/s)	Spot diameter (mm)	Overlap ratio	Defocus (mm)
2300	200	2	80%	18

ISSN: 2414-1895 DOI: 10.6919/ICJE.202501_11(1).0002

3. Experimental Results and Analysis

3.1 Phase Analysis

In order to explore the changes in the phase structure of the coating after the addition of Ti_2AlC, X-ray analysis was conducted on the coating, and the analysis results are shown in Fig. 2. According to Fig. 2, it can be observed that when the content of Ti_2AlC is 0%, both FCC and BCC phases exist in the CoCrFeNiTi coating, but the FCC phase dominates. This is because the atomic radii of CoCrFeNi in CoCrFeNiTi are similar, and they are more likely to combine with each other and form an FCC-structured solid solution, making the FCC structure dominate in the coating. With the addition of Ti_2AlC, the intensity of the main peak of the FCC phase decreases, and the other peaks of the FCC phase almost disappear. This may be caused by the solid solution strengthening effect of the new phases and other intermetallic compounds generated after adding Ti_2AlC to the CoCrFeNiTi high entropy alloy coating. After adding Ti_2AlC, new phases appear in the coating, such as a new close-packed hexagonal structure (HCP) and Ti_3AlC. Among them, Ti_2AlC may transform into Ti_3AlC under high temperature conditions. This is because during the laser cladding process, Ti_2AlC absorbs a large amount of heat. Under extremely high temperature conditions, some Ti atoms will migrate from Ti_2AlC to the Al layer, forming a new Ti_3AlC phase. Ti_2AlC and Ti_3AlC are two different MAX phase materials, and because the number and distribution of Ti-C bonds in the crystal structure of Ti_3AlC are different from those of Ti_2AlC, Ti_3AlC has better hardness and wear resistance than Ti_2AlC. As the content of Ti_2AlC continuously increases, new metal compounds are generated, causing the intensity of the main peak of the FCC phase to gradually decrease and even almost disappear.

In conclusion, when the content of Ti_2AlC is 0%, the coating is mainly dominated by the FCC phase. After adding Ti_2AlC, new HCP hexagonal phases and Ti_3AlC appear. The generation of new phases reduces the intensity of the characteristic peaks of the FCC phase. Moreover, under the action of high temperature, part of Ti_2AlC is transformed into Ti_3AlC. Therefore, the overall phase structure of the coating continuously adjusts with the increase in the content of Ti_2AlC.

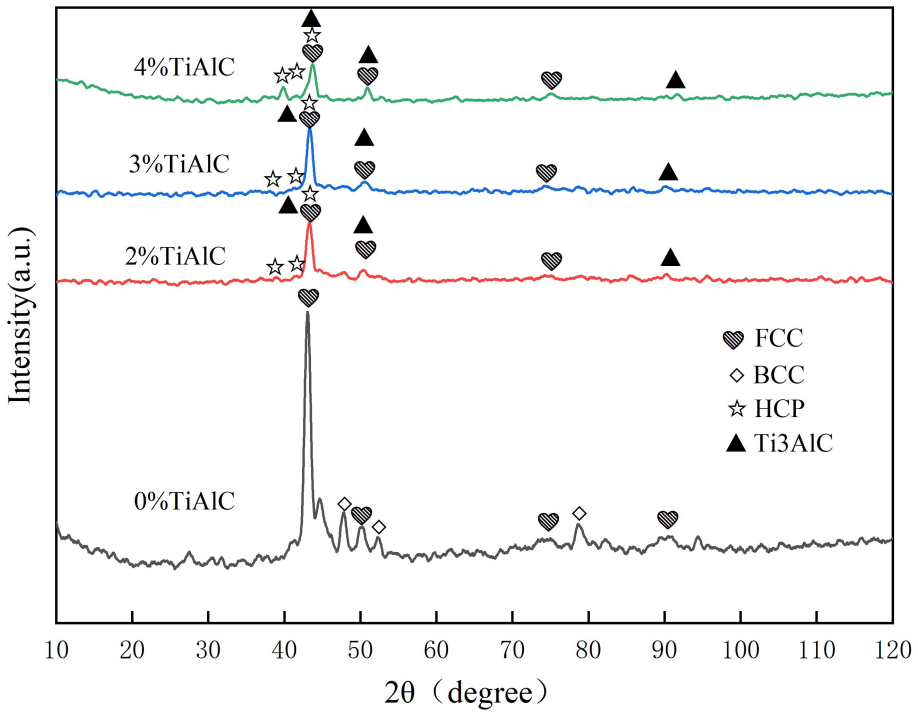

Fig. 2 XRD patterns of CoCrFeNiTi-(Ti_2AlC)x (x = 0%, 2%, 3%, 4%, wt%) coatings

ISSN: 2414-1895 DOI: 10.6919/ICJE.202501_11(1).0002

3.2 Microstructure

To further observe the changes in the microstructure and grain morphology of the coating after the addition of Ti_2AlC and to examine whether the addition of Ti_2AlC would affect the grain size of the coating, the scanning electron microscope was used to observe and detect the microstructure in the middle part of each coating. The specific results are shown in Fig. 3. The coating exhibits a relatively dispersed microstructure when the addition amount of Ti_2AlC therein is 0%. As shown in Fig. 3 (a), its grain state is characterized by relatively large cellular crystals and dendrites. With the addition amount of Ti_2AlC reaching 2%, a significant refinement occurs in the microstructure of the coating. As illustrated in Fig. 3(b), the grain state of the coating shifts from relatively large dendrites at an addition amount of 0% to smaller cellular crystals and dendrites. With the addition amount of Ti_2AlC reaching 3%, significant refinement characteristics are exhibited in the microstructure of the coating, as shown in Fig. 3(c). Compared to the coating with a Ti_2AlC content of 2%, the former exhibits a significant reduction in grain size, along with clearer grain boundaries and a significantly narrowed spacing between grain boundaries. As a result, the grains are distributed more densely and uniformly in space compared to the latter, demonstrating good microstructure characteristics, which is beneficial for improving the comprehensive performance of the coating. Moreover, at this time, unmelted Ti_2AlC particles were found in the coating (as shown in Fig. 4). To further confirm the existence of the lamellar metal compounds, EDS was used to conduct elemental analysis on these compounds, and the results are shown in Table 2. From the results, it can be observed that the element ratio basically conforms. The appearance of unmelted Ti_2AlC in the coating may be due to the fact that Ti_2AlC is coated with a dense Ni protective layer. During the cladding process, the Ni element on the surface maximally ensures that the intermediate Ti_2AlC is not melted and decomposed during the cladding process. It can also be observed from Fig. 3(c) that when the Ti_2AlC content is 3%, lamellar metal compounds were found in the coating (as shown in Fig. 5). To further confirm it, EDS was also used to conduct elemental analysis on it. Table 3 shows that its ratio roughly conforms to the ratio of Ti_3AlC. To further confirm whether it is Ti_3AlC, EDS was used to conduct area scanning analysis. From the color distribution in the results (Fig. 6), it can be observed that both Ti and Al elements exist. Combining with the previous XRD result analysis, it may be Ti_3AlC. When the Ti_2AlC content is 4%, the refinement effect on the microstructure of the coating is relatively low, and the grain composition in the microstructure of the coating changes from dendrites plus cellular crystals to cellular crystals plus a small amount of dendrites.

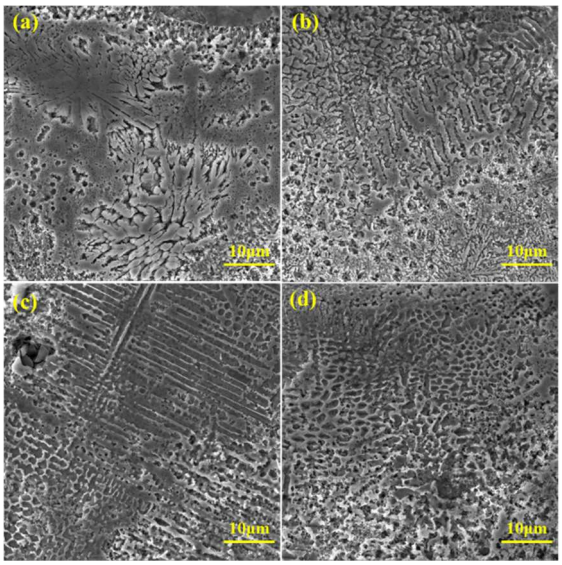

Fig. 3 Microstructures of coatings with different Ti_2AlC contents:
(a) 0%; (b) 2%; (c) 3%; (d) 4%

ISSN: 2414-1895 DOI: 10.6919/ICJE.202501_11(1).0002

In short, with the introduction of Ti_2AlC, the microstructure of the coating exhibits significant changes. Through observation with the scanning electron microscope, its microstructure has undergone an obvious refinement process, and characteristics such as grain morphology and size distribution have undergone substantial changes compared to when Ti_2AlC was not added. Specifically, the grain size is significantly reduced and the uniformity is significantly improved. Overall, the addition of Ti_2AlC has a practical and effective grain refinement effect on the microstructure of the coating, which is beneficial for optimizing the comprehensive performance of the coating.

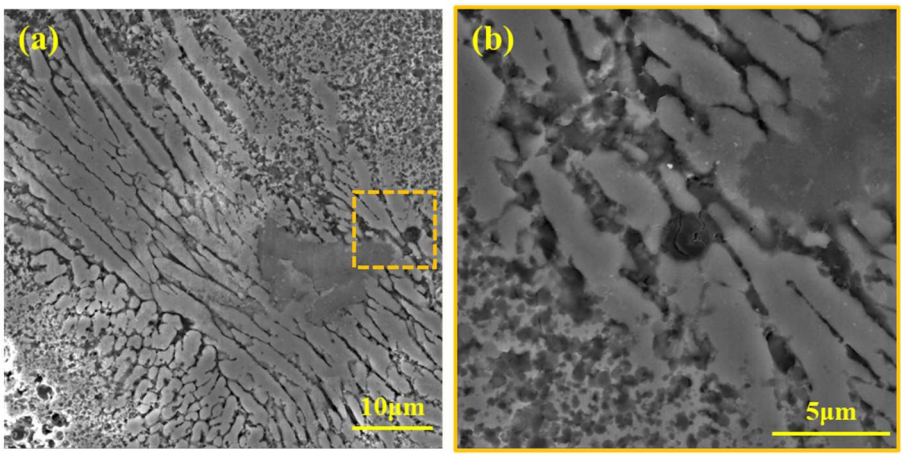

Fig. 4 Microstructure diagrams of 3% Ti_2AlC content

Table 2. EDS Spectral Analysis of 3% Ti_2AlC

Element	Ti	Al	C
wt%	31.69%	12.37%	55.65%

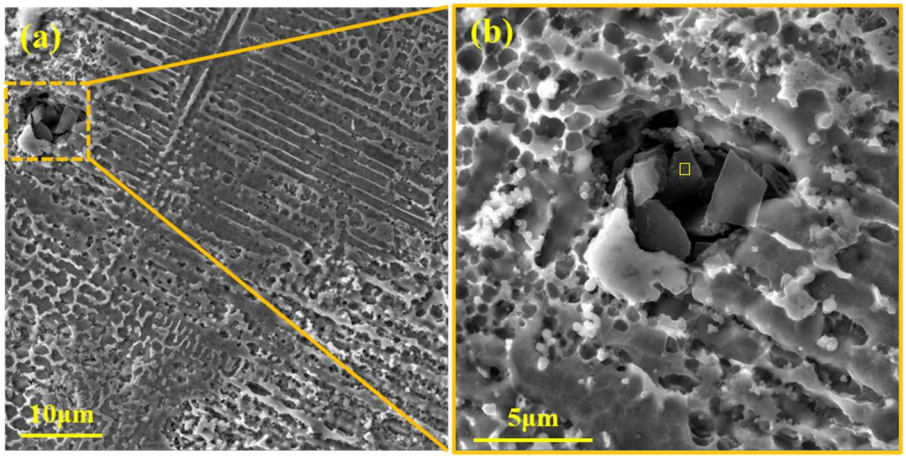

Fig. 5 Microstructure Diagram of 3% Ti_2AlC Content

Table 3. EDS Spectral Analysis of 3% Ti_2AlC

Element	Ti	Al	C
wt%	9.57	4.98	85.45

ISSN: 2414-1895 DOI: 10.6919/ICJE.202501_11(1).0002

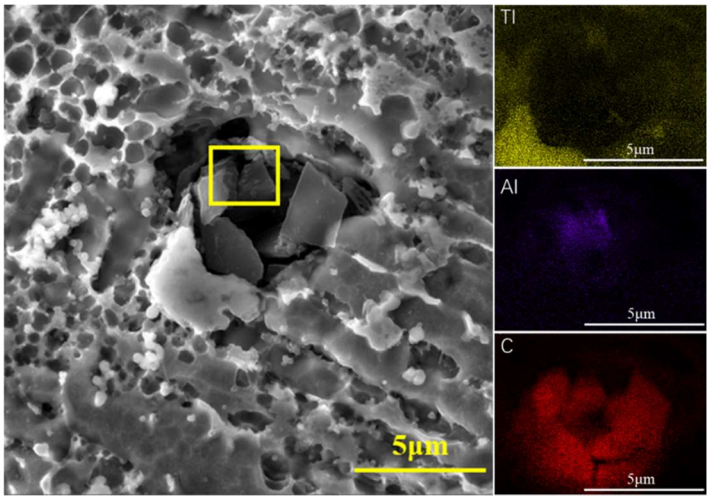

Fig. 6 Local Microstructure of CoCrFeNiTi-Ti_2AlC Coating

3.3 Modulus and Nanohardness

In order to further explore the influence law of the addition of Ti_2AlC on the mechanical properties of the coating, the mechanical properties of the coating were tested by using nano-indentation testing. The indentation morphology on the surface of the coating after the test is shown in Fig. 7. Since a triangular pyramid indenter is used in the nano-indentation test, triangular indentations appear on the surface of the coating. Through careful comparison and analysis, it is found that with the increase in the content of Ti_2AlC, the indentation volume and diameter of the coating show regular changes. When Ti_2AlC is not added (the content is 0%), the indentation diameter of the coating is relatively large. In order to compare the indentation depths corresponding to indenters with different indentation diameters, a visual display was made, and the results are shown in Fig. 8. When the content of Ti_2AlC is 0%, the indentation depth of the indenter reaches a peak value of 1212 nm, reflecting that the coating is relatively prone to plastic deformation at this time and has a weak ability to resist the indentation of external forces. When the content of Ti_2AlC is increased to 2%, the microstructure of the coating is optimized and adjusted, resulting in a significant reduction in the indentation volume, and the corresponding indentation depth of the indenter is reduced to 1086 nm, with a decrease rate of 10.4% (compared with that when the content is 0%), initially showing the improvement effect of Ti_2AlC on the mechanical properties of the coating. When Ti_2AlC is further increased to a content of 3%, the indentation volume of the coating continues to shrink, and the indentation depth is reduced to 989 nm. Compared with the content of 0%, the depth reduction rate is 22.55%. This fully indicates that the anti-deformation ability of the coating is significantly enhanced. The reason is that the incorporation of Ti_2AlC promotes the refinement of the internal microstructure of the coating and the reduction of grain size, enhancing the effect of grain refinement strengthening and enabling the coating to more effectively resist the indentation deformation under the action of external forces. However, when the content of Ti_2AlC is increased to 4%, the indentation volume of the coating does not show a significant further reduction, and the indentation depth of the indenter slightly rebounds to 1012 nm. It may be that more new phases are generated inside the coating at this content, resulting in an increase in the brittleness of the material and damage to the overall anti-deformation toughness, thereby weakening its resistance to the indentation of external forces.

In general, although there are local performance fluctuations at a high content (4%), overall, the appropriate addition of Ti_2AlC effectively improves the anti-deformation ability of the coating through the combined grain refinement effect caused by the new phase pinning effect, microstructure refinement, and grain size reduction.

ISSN: 2414-1895 DOI: 10.6919/ICJE.202501_11(1).0002

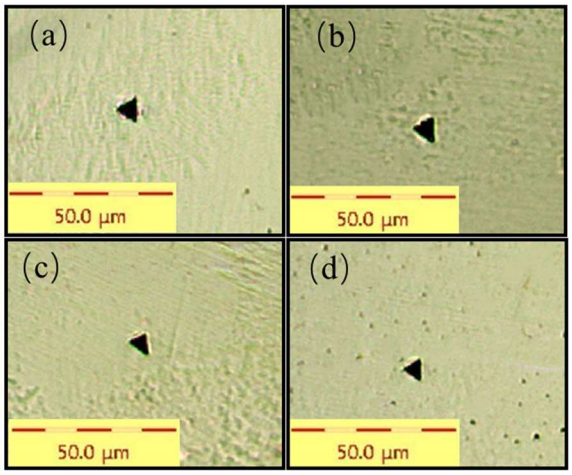

Fig. 7 Indentation Morphology of CoCrFeNiTi-Ti_2AlC Coating

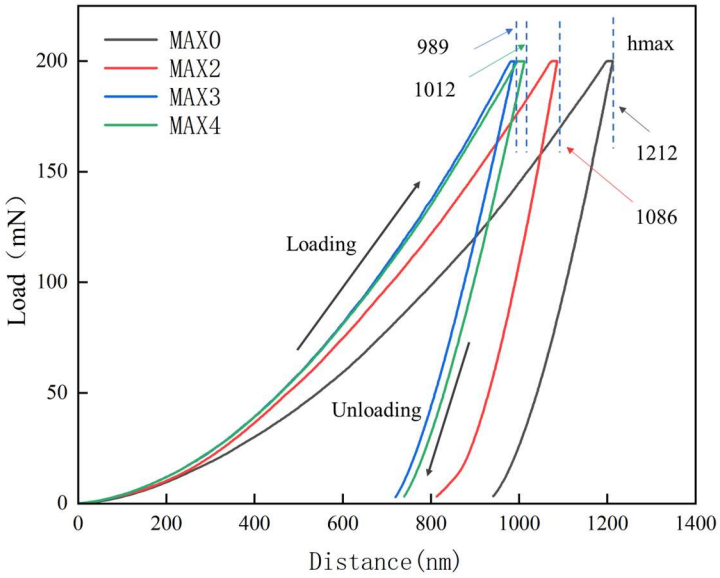

Fig. 8 Load-Displacement Curves of CoCrFeNiTi-Ti_2AlC Coating

After observing the changes in the indentation depth of the indenter, in order to analyze the influence of Ti_2AlC on the mechanical properties of the coating more deeply, the elastic modulus and average nano-hardness of the coating were obtained through indentation testing. The specific results are shown in Fig. 9. It can be observed from the figure that when the content of Ti_2AlC is 0%, the nano-hardness and elastic modulus of the coating are 8.65 Gpa and 204.06 Gpa, respectively. After Ti_2AlC is added to the coating, the nano-hardness and elastic modulus of the coating start to increase. When the content of Ti_2AlC increases to 2%, the nano-hardness of the coating increases to 11.2 Gpa, and the elastic modulus increases to 211.1 Gpa. This is due to the combined effect of the refinement of the coating's microstructure, the reduction in grain size, and the generation of new phases after the addition of Ti_2AlC, which leads to a slight improvement in the mechanical properties of the coating. When the content of Ti_2AlC increases to 3%, the nano-hardness of the coating is 12.57 Gpa, and the elastic modulus is 228 Gpa. The mechanical properties of the coating are the best when the content is 3%. Compared with when the content is 0%, the nano-hardness and elastic modulus of the coating are increased by 45.31% and 11.79%, respectively. According to the previous analysis, when the content is 3%, the refinement degree of the coating's microstructure is relatively high, and the grains are distributed uniformly and densely. Eventually, under the synergistic effect of the grain refinement strengthening and the pinning effect of the newly generated phases, the mechanical properties of the coating are effectively improved. However, when the content of Ti_2AlC increases to 4%, both the

ISSN: 2414-1895 DOI: 10.6919/ICJE.202501_11(1).0002

nano-hardness and elastic modulus of the coating decrease to varying degrees. The nano-hardness of the coating decreases to 208.92 Gpa, and the elastic modulus decreases to 11.16 Gpa. According to the previous analysis, the decline in the coating's performance may be due to the generation of more new phases inside the coating, resulting in an increase in the brittleness of the material and ultimately leading to a decline in the coating's performance. Overall, the mechanical properties of the coating have been significantly improved after the addition of Ti_2AlC.

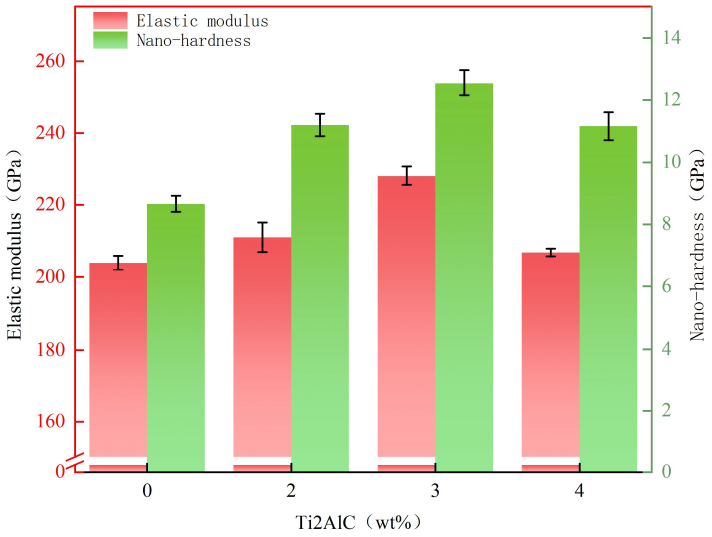

Fig. 9 Average Elastic Modulus and Average Nano-hardness of CoCrFeNiTi-Ti_2AlC Coating

3.4 Friction Wear Resistance

In order to further explore the wear resistance of the coating and the self-lubricating property of Ti_2AlC, a friction and wear test was conducted on the coating. The changes in the friction coefficient of the coating are shown in Fig. 10. It can be observed from Fig. 10 that after Ti_2AlC is added to the coating, the friction coefficient of the coating decreases as the content of Ti_2AlC increases. To present the changes in the wear track morphology and wear depth of the coating after the addition of Ti_2AlC more intuitively, the macroscopic morphology of the wear track and the wear depth were analyzed, and the results are shown in Fig. 11. The following will analyze the influence of Ti_2AlC on the wear resistance of the coating by combining the changes in the friction coefficient of the coating, the wear morphology of the coating, and the changes in the wear track depth. When the content of Ti_2AlC is 0%, the friction coefficient of the coating is 0.528, indicating that the wear resistance of the coating is relatively poor when Ti_2AlC is not added. Combined with the macroscopic appearance of the wear track (Fig. 11(a)), it can be seen that the wear track of the coating is the deepest and relatively wide at this time. Based on the conclusions in the previous study, the reason for the relatively high friction coefficient of the coating is that the coating only relies on its own high hardness and the oxide film formed during the friction process to protect the substrate. There is no lubricating phase acting on the surface of the coating during the mating process of the friction pair and the coating, so the friction coefficient of the coating is relatively high. When the content of Ti_2AlC is 2%, under the dual effects of grain refinement strengthening and the pinning effect, the hardness of the coating is significantly improved. According to Archard's theorem, the hardness of the coating is positively correlated with the wear resistance, so the wear resistance of the coating is also improved, and the friction coefficient of the coating decreases to 0.481 (Fig. 10). When the content of Ti_2AlC is 3% (Fig. 11(c)), the width of the wear track of the coating becomes narrower. By observing the curve of the change in the wear track depth (Fig. 11(e)), it can be seen that the wear depth of the coating becomes significantly shallower. Compared with when the content is 0%, the friction coefficient of the coating reaches the lowest value of 0.457, the wear condition of the coating is relatively uniform at this time, and the wear depth of the coating reaches the lowest value. According to the previous analysis, there are two

ISSN: 2414-1895 DOI: 10.6919/ICJE.202501_11(1).0002

reasons for the improvement in the wear resistance of the coating. Firstly, it is caused by the relatively high hardness of the coating at this time. According to Archard's theorem, the high hardness of the coating can improve its wear resistance. Secondly, when the content of Ti_2AlC is 3%, unmelted Ti_2AlC and lamellar Ti_3AlC are found in the coating. Under the self-lubricating effect of Ti_2AlC, the effect of reducing friction is achieved.

To further illustrate the role of Ti_2AlC in reducing friction during the friction process, Fig. 12 shows the friction reduction mechanism of Ti_2AlC from a microscopic perspective. As shown in the diagram, due to the special layered structure of Ti_2AlC, the interlayer bonding force is relatively weak, and relative sliding between the layers is likely to occur under the action of friction heat and pressure. This sliding process is similar to solid lubrication and can provide good lubricating performance without introducing a liquid lubricant. Therefore, as the friction progresses, some Ti_2AlC particles will gradually accumulate at the friction interface and form a continuous lubricating film. This lubricating film can effectively separate the two friction surfaces and reduce the direct contact between metals, thereby reducing the friction coefficient and further improving the wear resistance of the coating. When the content of Ti_2AlC is 4%, the friction coefficient of the coating is 0.497, and the wear resistance has a certain decline compared with that when the content is 3%. Moreover, the wear track of the coating becomes rough at this time, and the wear depth has a slight rebound compared with that when the content is 3%. According to the previous analysis, the reason for the decline in wear resistance when the content is 4% may be that too many new phases are generated in the coating when the content of Ti2AlC is at this level. This leads to an increase in the brittleness of the coating and, consequently, a decline in the wear resistance. To put it briefly, although there is some fluctuation in the wear resistance of the coating when the content of Ti_2AlC is 4%, the addition of Ti_2AlC does significantly improve the wear resistance of the coating and plays a role in reducing friction in the coating.

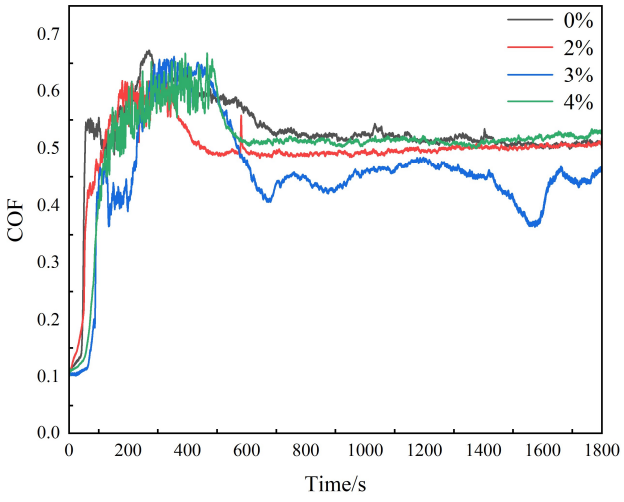

Fig. 10 Friction Coefficient Diagram of CoCrFeNiTi-Ti_2AlC Coating

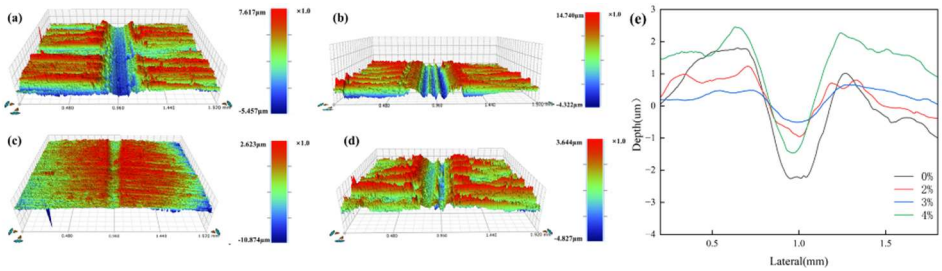

Fig. 11 The 3D morphologies of the wear tracks of the CoCrFeNiTi-Ti_2AlC Coating

ISSN: 2414-1895 DOI: 10.6919/ICJE.202501_11(1).0002

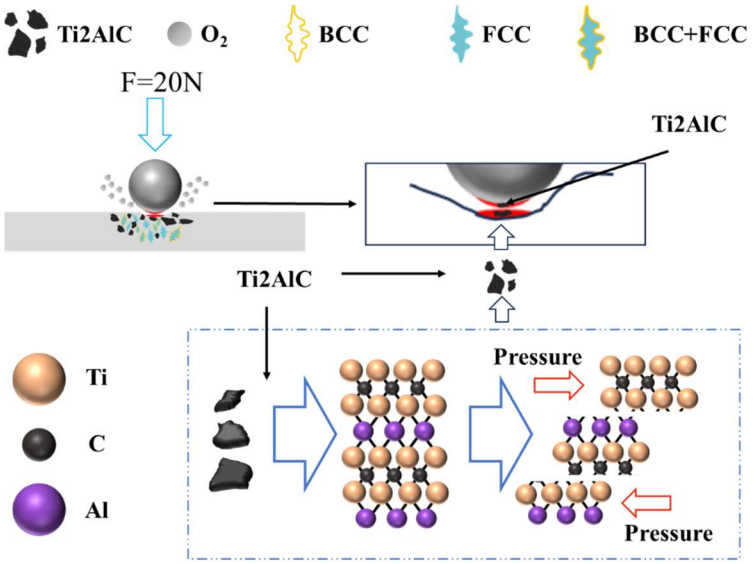

Fig. 12 Wear Mechanism Diagram of CoCrFeNiTi-Ti_2AlC Coating

4. Conclusion

After a series of rigorous experiments and meticulous observational analyses, pivotal conclusions about the impact of Ti2AlC on the performance of coatings have been drawn. These conclusions clearly illustrate the unique effectiveness of Ti2AlC in the coating system in multiple aspects, ranging from microstructure to mechanical and tribological properties. The specific conclusions are as follows:

(1) When the content of Ti_2AlC is 0%, the coating is mainly dominated by the FCC phase. After adding Ti_2AlC, new HCP hexagonal phases and Ti_3AlC appear. The generation of new phases reduces the intensity of the characteristic peaks of the FCC phase. Moreover, after Ti_2AlC is added to the coating, the microstructure of the coating is significantly refined. When the content of Ti2AlC reaches 3%, the optimal effect is achieved. Compared with when the content is 0%, the grain size is smaller, the grain boundaries are clearer, the spacing between grain boundaries is significantly narrowed, and the grain distribution is more compact and uniform.

(2) The mechanical properties of the coating have been significantly improved after adding Ti_2AlC. The coating demonstrates its peak performance at a Ti_2AlC content of 3%, as opposed to the case where Ti_2AlC is not incorporated (with a Ti_2AlC content of 0%). The indentation depth of the coating decreases from 1212 nm to 989 nm, with a decrease rate of 22.55%. The elastic modulus increases from 204.06 Gpa to 228 Gpa, and the nano-hardness increases from 8.65 Gpa to 12.57 Gpa, with the increase rates being 45.31% and 11.79%, respectively.

(3) Due to the generation of new phases that improve the hardness of the coating, the self-lubricating material Ti_2AlC plays a good role in reducing friction during the friction process, making the wear resistance of the coating reach the best when the content of Ti_2AlC is 3%. The wear track is narrow and shallow, and the wear is uniform. The friction coefficient decreases from 0.528 when the content is 0% to 0.481. Compared with when Ti_2AlC is not added, both the width of the wear track and the wear depth are significantly reduced.

References

[1] LIU Y N, DING Y, YANG L J, et al. Research and progress of laser cladding on engineering alloys: A review[J]. Journal of Manufacturing Processes, 2021, 66: 341-363.

[2] XIANG D D, LIU Y S, YU T B, et al. Review on wear resistance of laser cladding high-entropy alloy coatings[J]. Journal of Materials Research and Technology, 2024, 28: 911-934.

[3] ZHU L D, XUE P S, LAN Q, et al. Recent research and development status of laser cladding: A review[J]. Optics & Laser Technology, 2021, 138: 106915.

ISSN: 2414-1895 DOI: 10.6919/ICJE.202501_11(1).0002

[4] ZHANG P, LI Z W, LIU H M, et al. Recent progress on the microstructure and properties of high entropy alloy coatings prepared by laser processing technology: A review[J]. Journal of Manufacturing Processes, 2022, 76: 397-411.

[5] ZHONG M, LIU W. Laser surface cladding: The state of the art and challenges[J]. Proceedings of the Institution of Mechanical Engineers, Part C: Journal of Mechanical Engineering Science, 2010, 224(5): 1041-1060.

[6] WEN X, CUI X F, JIN G, et al. Corrosion and tribo-corrosion behaviors of nano-lamellar Ni1.5CrCoFe0.5Mo0.1Nbx eutectic high-entropy alloy coatings: The role of dual-phase microstructure[J]. Corrosion Science, 2022, 201: 110305.

[7] GUAN Y J, CUI X J, CHEN D, et al. Realizing high strength and toughness of gradient high-entropy alloy coating by in-situ interface reaction of FeCoCrNi/FeCoCrAl[J]. Surface and Coatings Technology, 2023, 464: 129569.

[8] LIANG Y, LIAO Z Y, ZHANG L L, et al. A review on coatings deposited by extreme high-speed laser cladding: processes, materials, and properties[J]. Optics & Laser Technology, 2023, 164: 109472.

[9] SCHOPPHOVEN T, GASSER A, BACKES G. EHLA: Extreme High-Speed Laser Material Deposition[J]. Laser Technik Journal, 2017, 14(4): 26-29.

[10] SCHOPPHOVEN T, GASSER A, WISSENBACH K, et al. Investigations on ultra-high-speed laser material deposition as alternative for hard chrome plating and thermal spraying[J]. Journal of Laser Applications, 2016, 28(2): 022501.

[11] XIAO Q, XIA J L, GAO X S, et al. Investigation of the Microstructure and Wear Properties of Conventional Laser Cladding and Ultra-High-Speed Laser Cladding Alloy Coatings for Wheel Materials[J]. Coatings, 2023, 13(5): 949.

[12] MENG L, ZHU B B, LIU X, et al. Comparison on the Ni60 Coatings Deposited by Extreme-High-Speed and Conventional Laser-Induction Hybrid Cladding Technologies: Forming Features, Microstructure and Wear Behaviors[J]. Metallurgical and Materials Transactions A, 2023, 54(8): 3118-3133.

[13] YEH J W, CHEN S K, LIN S J, et al. Nanostructured High-Entropy Alloys with Multiple Principal Elements: Novel Alloy Design Concepts and Outcomes[J]. Advanced Engineering Materials, 2004, 6(5): 299-303.

[14] YEH J W. Recent progress in high-entropy alloys[J]. European Journal of Control - EUR J CONTROL, 2006, 31: 633-648.

[15] JIN B Q, ZHANG N N, YU H S, et al. AlxCoCrFeNiSi high entropy alloy coatings with high microhardness and improved wear resistance[J]. Surface and Coatings Technology, 2020, 402: 126328.

[16] LI Y Y, LIU H, LIU X H, et al. Microstructure, thermostability and tribological behavior of composite CoCrFeNiTix high-entropy alloy coatings fabricated by laser cladding[J]. Optik, 2023, 283: 170899.

[17] WANG X Y, LIU Q, HUANG Y B, et al. Effect of Ti Content on the Microstructure and Corrosion Resistance of CoCrFeNiTix High Entropy Alloys Prepared by Laser Cladding[J]. Materials, 2020, 13(10): 2209.

[18] ZHOU J li, CHENG Y hai, YANG J yong, et al. Effects of WS2 and Ti3AlC2 additions on the high temperature wear properties of laser cladding YW1/NiCoCrAlY tool coating[J]. Ceramics International, 2021, 47(24): 35124-35133.

[19] LI X, ZHANG C H, ZHANG S, et al. Manufacturing of Ti3SiC2 lubricated Co-based alloy coatings using laser cladding technology[J]. Optics & Laser Technology, 2019, 114: 209-215.